



RESEARCH ARTICLE - ENGINEERING

Speed Control Using an Integral Sliding Mode Controller for a Three-Phase Induction Motor

Samar AL-Hashemi^{1*}, Ayad AL-Dujaili¹, Ahmed R. Ajel¹

¹ Electrical Engineering Technical College, Middle Technical University, Baghdad, Iraq.

* Corresponding author E-mail: samar88alhashimi@gmail.com

Article Info.	Abstract
<p><i>Article history:</i></p> <p>Received 09 May 2021</p> <p>Accepted 28 July 2021</p> <p>Publishing 30 September 2021</p>	<p>Induction motors are widely used in commercial and industrial applications due to their robustness, high efficiency, low maintenance requirements and durability among other reasons. Consequently, their speed should be controlled for better performance. This paper describes utilization of a scalar speed control of a three-phase squirrel cage induction motor (SCIM) to control a motor's speed using an integral sliding mode controller (ISMC). The controller was tested under various operating conditions. The results are compared with a case employing a conventional PI controller. It was found that speed control by ISMC has a 0.16 RPM steady-state error, 0.03 s to reach steady-state from a standstill, and a 5% overshoot. All of these are lower values as compared to the results of a conventional PI controller. In this paper, the robustness of each controller to uncertainties is checked. Simulation results show the advantages of ISMC control methods. The system is simulated using MATLAB SIMULINK R2017a.</p>

2019 Middle Technical University. All rights reserved

Keywords: Control, Integral; Induction Motor; Inverter; Sliding Mode; Speed; Three-phase

1. Introduction

Since induction motors are inexpensive, well-constructed, robust and require little maintenance, they are widely used in industrial applications and manufacturing processes [1]. In the last few decades, the developments of electrical drives contributed to increasing the usability of induction motors [2]. If a three-phase induction motor is powered by the mains of a three-phase source, then its rotational speed will be equivalent to the synchronous speed during loading or unloading processes. Sometimes it is required to control the speed of this motor over a high range of speeds to levels more than the synchronous speed. For this purpose, an inverter is used. An inverter has the ability to supply variable voltages and frequencies. Decisions about the values of these voltages and frequencies are made through a controller [3]. There are various kinds of controllers that can be employed for three-phase motors. They include scalar (V/F) control or vector control which includes field-oriented control (FOC) and direct torque control (DTC) [4]. In contrast with vector control, scalar control is simple which makes it widely employed in many applications [5]. In this technique, various kinds of controllers can be used including PI, fuzzy logic, and sliding mode controllers, among others. Numerous researchers have published their results for accomplishing speed control of three-phase induction motors. Venkateswarlu et al. [6] controlled the speed of a three-phase induction motor with a sliding mode controller (SMC). Using this method, control is made using no sensor, but instead observation of stator and rotor flux was employed. Also, SMC was used by El-gendy et al. [7] for speed control, as well, using a (V/F) method. A space vector modulation technique was also used. The performance of SMC via the scalar method was compared with a PI controller. Pati et al. [8] used SMC with a scalar method to improve the transient response of a motor. SMC performance was compared with a PI controller. An adaptive SMC with fuzzy logic controller (FLC) was used by Zeb et al. [9]. They employed the scalar method as well, where the FLC was based on the steepest descent with adaptive SMC. The controller performance was compared with a PI controller. Yaseen and Nasser [10] used SMC for speed control of a three-phase induction motor. They proposed estimation of the frequency of stator voltage, whereas the slip speed was based on a quadratic function of current.

Nomenclature			
DTC	Direct Torque Control	ISMC	Integral Sliding Mode Controller
FLC	Fuzzy Logic Controller	PWM	pulse width modulation
FOC	Field - Oriented Control	SCIM	3-phase Squirrel Cage Induction Motor
Symbols			
V	Voltage	ω_r	Electrical speed of the rotor
n_s	Synchronous speed	H	Inertia
f	Supply frequency	T _m	Mechanical torque
p	Number of poles	T _e	Electrical torque
ω_s	Synchronous angular speed	M _i	Modulation index
ω_m	Mechanical speed of the motor	A _r	Peak amplitude of Reference sine signal
ω_{slip}	Slip speed	A _c	Peak amplitude of the triangle carrier signal
ω_e	Rotational electrical frequency	(Δe) or (\dot{e})	Change of error
i	Current	σ	Sliding surface
r	Leakage resistance	s	Auxiliary sliding variable
φ	Flux linkage	z	Uncertainty

Their proposed control method was compared with a PI controller. For inverter modulation with scalar speed control, a comparison of various pulse width modulation (PWM) techniques was done by Divyam et al. [11]. Comparison was made between space vector PWM, sinusoidal PWM, and multiple PWM. The current work examines speed control of a three-phase squirrel cage induction motor (SCIM). Speed is controlled using an integral sliding mode controller (ISMC). This paper is organized as follows: An introduction is given, followed by a system description, speed control of three-phase induction motor, simulation results and conclusions.

2. System Description

Normally, a system consists of a three-phase squirrel cage induction motor (SCIM) supplied with AC voltage through a three-phase inverter. The supply voltage of the inverter is DC, which can originate from either a battery or rectified AC from a three-phase or single-phase source. A tachometer or speedometer was used to measure the rotational speed of the motor. A description of the main parts of the system are given in the following sub-sections.

2.1. Three-Phase SCIM

There are two types of induction motors, wound rotor and squirrel cage types. An SCIM does not contain rotor windings. Instead, the rotor is constructed from steel bars that are short-circuited from its terminals. Thin disks are merged between the terminals and held together to form a laminated cross-section. The advantage of this laminated structure is a reduction of eddy currents. Owing to this construction, an SCIM does not require periodic maintenance since it does not have brushes or slip rings [12]. Thus, SCIMs are often employed in many industrial, dusty, and greasy environments. If the motor is supplied by a main voltage and frequency, then its speed will not exceed the synchronous speed. The synchronous speed (n_s) is the speed of the rotating magnetic field between stator and rotor as:

$$n_s = \frac{120 \times f}{P} \quad (1)$$

where f is the supplied frequency, and P is the number of poles. Also, n_s can be represented as angular speed ω_s where:

$$\omega_s = \frac{2\pi n_s}{60} \quad (2)$$

All electrical parameters are referenced to the stator [12]. Each value of stator and rotor parameters can be analysed as (d - q) expressed as follows [13-14, 8]:

$$V_{ds} = r_s i_{ds} + \frac{d}{dt} \varphi_{ds} - \omega_s \varphi_{qs} \quad (3)$$

$$V_{qs} = r_s i_{qs} + \frac{d}{dt} \varphi_{qs} + \omega_s \varphi_{ds} \quad (4)$$

$$\dot{V}_{dr} = r'_r i'_{dr} + \frac{d}{dt} \varphi'_{dr} - (\omega_s - \omega_r) \dot{\varphi}_{qr} \quad (5)$$

$$\dot{V}_{qr} = r'_r i'_{qr} + \frac{d}{dt} \varphi'_{qr} + (\omega_s - \omega_r) \dot{\varphi}_{dr} \quad (6)$$

where the suffixes, s and r, refer to stator and rotor, respectively, while d & q refer to direct and quadrature axes, respectively. V represents voltage, i is current, r is leakage resistance, and φ is flux linkage. ω_r represents the electrical speed of the rotor. The acute accented variables in Eq. 5-6 refer to the rotor referenced to the stator. Electromagnetic torque (T_e) is calculated as:

$$T_e = 1.5 P (\varphi_{ds} i_{qs} - \varphi_{qs} i_{ds}) \quad (7)$$

The dynamic mathematical equations of a SCIM are represented via a synchronous rotating reference frame. φ is represented as:

$$\varphi_{ds} = L_s i_{ds} + L_m i'_{dr} \quad (8)$$

$$\varphi_{qs} = L_s i_{qs} + L_m i'_{qr} \quad (9)$$

$$\varphi'_{dr} = L_r i'_{dr} + L_m i_{ds} \quad (10)$$

$$\varphi'_{qr} = L_r i'_{qr} + L_m i_{qs} \quad (11)$$

The mechanical system of a SCIM is given by the following equation:

$$\frac{d}{dt} \omega_m = \frac{1}{2H} (T_e - \omega_m - T_m) \quad (12)$$

where H represents inertia, ω_m and T_m are mechanical speed and torque of the motor, respectively. All of the above equations are used to design a dynamic model of a three-phase SCIM.

2.2. Three-phase inverter

An inverter is DC/AC converter that changes a supplied DC voltage into an AC voltage at a desired amplitude and frequency. A three-phase inverter has three legs. Each leg has two switching devices that are normally MOSFETs or IGBTs. The upper switches are responsible for positive polarity, while the lower switches are responsible for the negative polarity of the three-phase output voltage. The output line to line voltages are represented as [15]:

$$v_{ab} = \sum_{n=1,3,5,\dots}^{\infty} \frac{4V_{DC}}{n\pi} \sin\left(\frac{n\pi}{2}\right) \sin\frac{n\pi}{3} \sin n\left(\omega t + \frac{\pi}{6}\right) \quad (13)$$

$$v_{bc} = \sum_{n=1,3,5,\dots}^{\infty} \frac{4V_{DC}}{n\pi} \sin\left(\frac{n\pi}{2}\right) \sin\frac{n\pi}{3} \sin n\left(\omega t - \frac{\pi}{2}\right) \quad (14)$$

$$v_{ca} = \sum_{n=1,3,5,\dots}^{\infty} \frac{4V_{DC}}{n\pi} \sin\left(\frac{n\pi}{2}\right) \sin\frac{n\pi}{3} \sin n\left(\omega t - \frac{7\pi}{6}\right) \quad (15)$$

Modulation techniques are used to reduce harmonics and attain a smooth AC voltage. The modulation technique employed in this work is sinusoidal pulse width modulation (SPWM). Three pure sine waves shifted by 120° are considered as modulating (reference) signals at the desired frequency. These signals are compared with a triangle carrier at a high frequency. The root mean square (RMS) value of the output voltage is regulated by varying the modulation index (M_i), which can be calculated as:

$$M_i = \frac{A_r}{A_c} \quad (16)$$

where A_r and A_c are the peak amplitude of a reference sine signal and triangle carrier, respectively. The simulation model of the modulation portion of the system was done using MATLAB Simulink as depicted in Fig. 1:

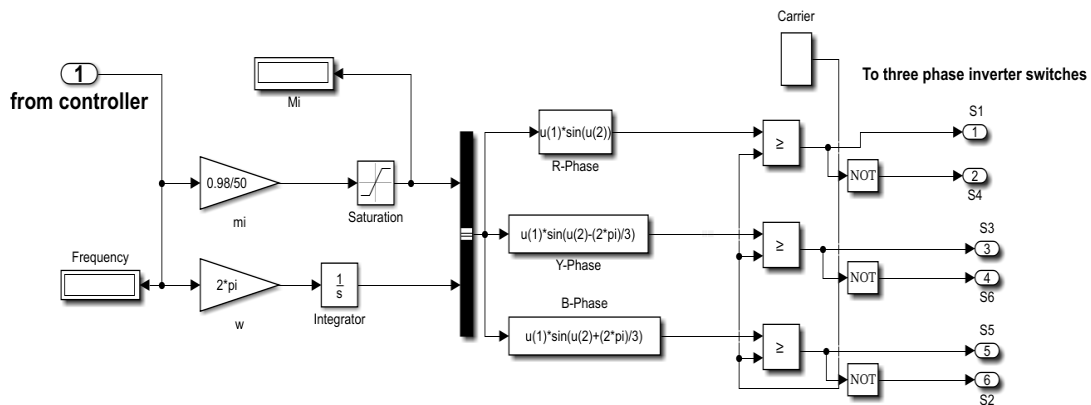


Fig. 1 Simulation model of inverter modulation

3. Speed Control of Three-Phase Induction Motor

One technique that can be used to control the speed of a three-phase SCIM is stator voltage and frequency control, otherwise known as the scalar (V/F) method. This technique requires a three-phase inverter supplied by a constant DC voltage with the capability of regulating its output voltage and frequency. Voltage regulation is done by controlling the modulation index. Frequency regulation is accomplished by controlling the frequency of the three modulating signals. In the (V/F) method, the maximum torque (T_{max}) of the motor is kept at a constant value for speeds ranging between 10-15% of its ω_s and up to ω_s . For speeds greater than ω_s , T_{max} will start to decrease. Then, the load torque should be reduced accordingly to maintain the required speed of the motor. In this work, the speed of the three-phase SCIM is controlled using the (V/F) technique via use of the controllers described in the proceeding sub-sections.

3.1. Speed control using a PI controller

Speed control using a proportional integral (PI) controller is done by calculating the error (e) between measured speed ω_m and the desired set point ω_m^* where:

$$e = \omega_m^* - \omega_m \quad (17)$$

In any control method, should be zero at a steady-state condition. The generated e is fed to PI controller where a controlling variable $u(t)$ is generated such that:

$$u(t) = e(t) \times KP + \frac{KI}{TI} \int e(t)dt \quad (18)$$

where KP and KI are the proportional and integral gains of the PI controller [16]. These gains can be set or tuned to attain the required response of the system. The controller generates the slip speed ω_{slip} signal that is added with ω_m that yields synchronous speed ω_e . Fig. 2 represents speed control of a three-phase SCIM by a PI controller.

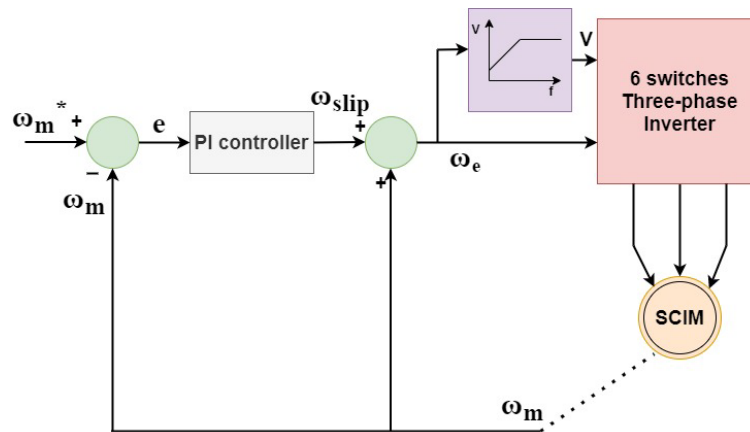


Fig. 2 Speed control of a three-phase SCIM by a PI controller

In this figure, the difference between ω_m^* and ω_m represents an error (e). $u(t)$ represents ω_{slip} , which is added to ω_m to get ω_e . Then, ω_e represents the rotational electrical frequency where the supply frequency can be extracted. In this case, the supply frequency may vary depending on the action of the PI controller. According to the supplied frequency, the resulting modulation index is calculated through a linear relationship between them it and then fed along with frequency to a three-phase inverter.

3.2. Speed control by an integral sliding mode control (ISMC)

Sliding mode control (SMC) is a robust, nonlinear and discontinuous control technique. It has the capability to slide the system states on a particular surface in a state-space environment. The trajectory of the system states is called a sliding surface [17]. In SMC, system state variables are near the sliding surface [18]. The sliding surface is defined using a surface equation (σ) such that:

$$\sigma = \dot{e} + ce \quad (19)$$

where c is a constant and always > 1 , e represents the error as a state variable, \dot{e} is the change of e with respect to time. The aim of SMC is to drive σ to a value of zero. An integral sliding mode controller (ISMC) is used to compensate for system disturbances without the existence of a reaching phase [19]. This objective is achieved when the equivalent control variable $u_2(t)$ is equal to -1 multiplied by (z). Thus, the auxiliary sliding variables are defined as:

$$s = \sigma - z \quad (20)$$

$$\dot{z} = -1 \times u_2(t) \quad (21)$$

where z represents uncertainty. In order to complete the controller design, then:

$$u_2(t) = k \times \sigma \quad (22)$$

Here, k is a constant > 1 . Now, $u_1(t)$ is a nominal control variable that is used to drive auxiliary sliding variables to zero where:

$$u_1(t) = \rho \times \text{signs}(s) \quad (23)$$

and ρ represents a control parameter. Finally, the controlling signal $u(t)$ is defined by the following formula:

$$u(t) = u_1(t) + u_2(t) \quad (24)$$

Speed control of a three-phase SCIM is done using ISMC through definition of state variables that include error (e) and change of error (\dot{e}), as is shown in Fig. 3.

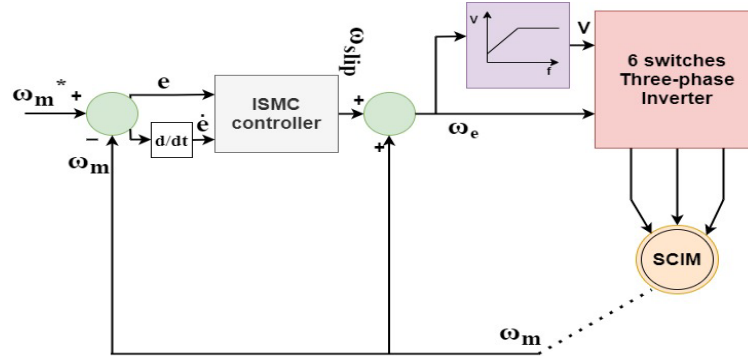


Fig. 3 Speed control of a three-phase SCIM by ISMC

4. Simulation Results

Operation of the SCIM was simulated using MATLAB Simulink R2017a. The suggested ISMC controller was simulated as shown in fig. 4 and, in parallel, a PI controller was also simulated for comparison. The parameters used in the SCIM of this paper are listed in the Table 1. Various simulations were done according to the cases presented in the following sub-sections to elucidate the speed control and system behaviour.

4.1. System response at the start

The desired speed reference was 1000 RPM or 104.71 rad per second. At the beginning, a PI controller was used. Fig. 5 shows a high overshoot and delay time compared to ISMC, which will subsequently be used. In the ISMC case, the simulation results show a rapid response to reach a steady-state condition with a lower overshoot value. Fig. 6 represents the system trajectory of error (e) and change of error (Δe , or \dot{e}) when ISMC is used. The speed of the motor starts from zero until reaching steady state at the desired set point. In comparison with Figure (5), the motor speed decreases for a short period of time, then the motor accelerates towards the set point.

Table 2 represents both controller responses. The gains of the PI controller were set after tuning. They were $k_p = 0.01$ and $K_i = 0.3$.

Table 1 SCIM parameters

Parameters	Values
Rated Voltage	400 V line to line
Input Power	4 kW
Output power	5.4 hp
Frequency	50 Hz
Rated Speed	1430 RPM
Stator Resistance	1.405 Ω
Stator Inductance	0.005839 H
Rotor Resistance	1.395 Ω
Rotor Inductance	0.005839 H
Mutual Inductance	0.1722 H
Inertia	0.0131 J(kg.m ²)
No. of poles	4

Table 2 Speed response for the controllers

	Overshoot (%)	Steady state Time (s)	Steady state error (RPM)
PI	44	0.26	6
ISMC	5	0.03	0.16

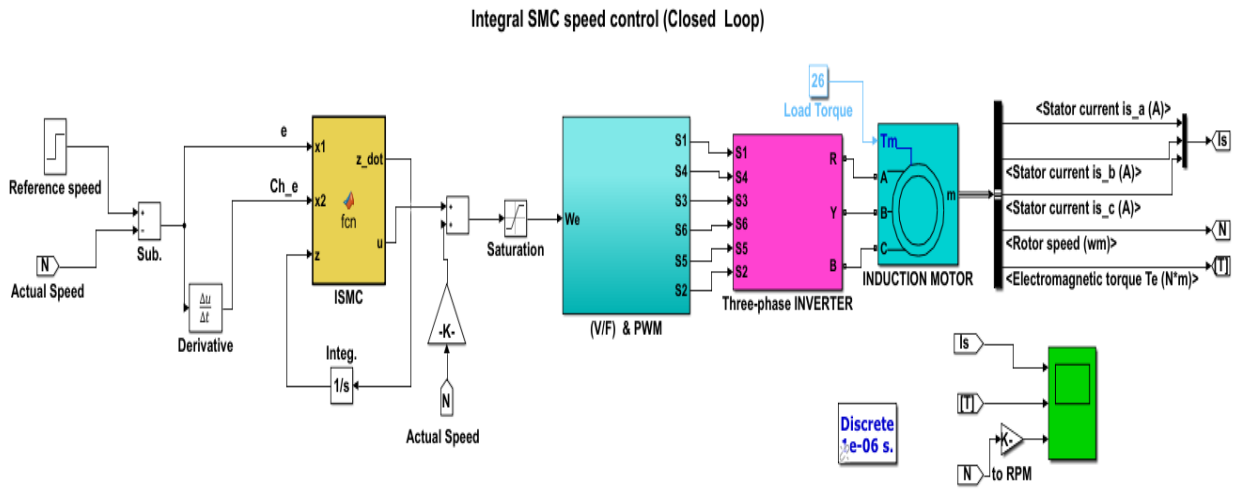


Fig. 4 System simulation by MATLAB Simulink when ISMC is used

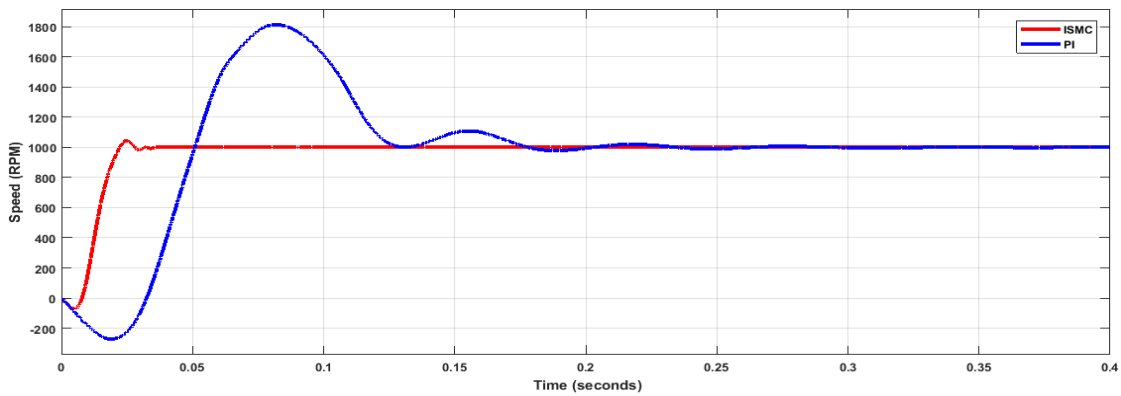


Fig. 5 Speed control response of SCIM by PI and ISMC

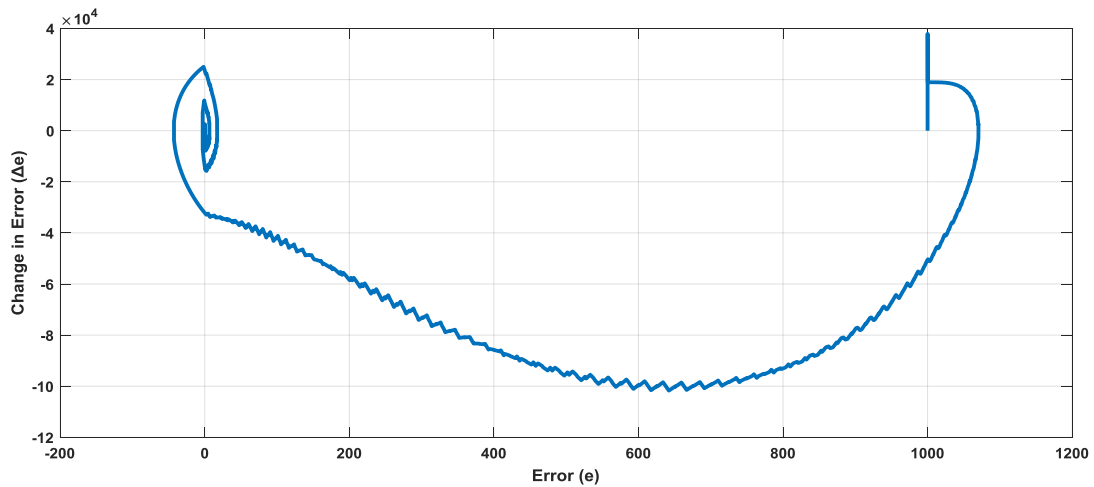


Fig. 6 Trajectory of e and (\dot{e})

4.2. System response to change in the desired speed

In this case, the motor load torque is kept constant at its rated value. The speed of the motor changes from 700 RPM to 1200 RPM. When a PI controller is used, during speed change, the simulation results show a clear overshoot in the speed response and electrical torque (T_e) of the motor, as shown in Fig. 7. During this transient period, which lasted for 0.08 seconds, the T_e of the motor reached more than twice its rated value. Also, the speed overshoot is high, but less than shown in Fig. 5. This is due to the low-speed differences in the cases examined. Simulation

results when ISMC is used are shown in Fig. 8. In this case, the transient period lasted to 0.02 seconds with low overshoot in the speed response. In this short period, the T_e of the motor was high, reaching approximately five times its rated value. However, this high change might not affect the motor operation or the entire system due to the very short duration of this transient period.

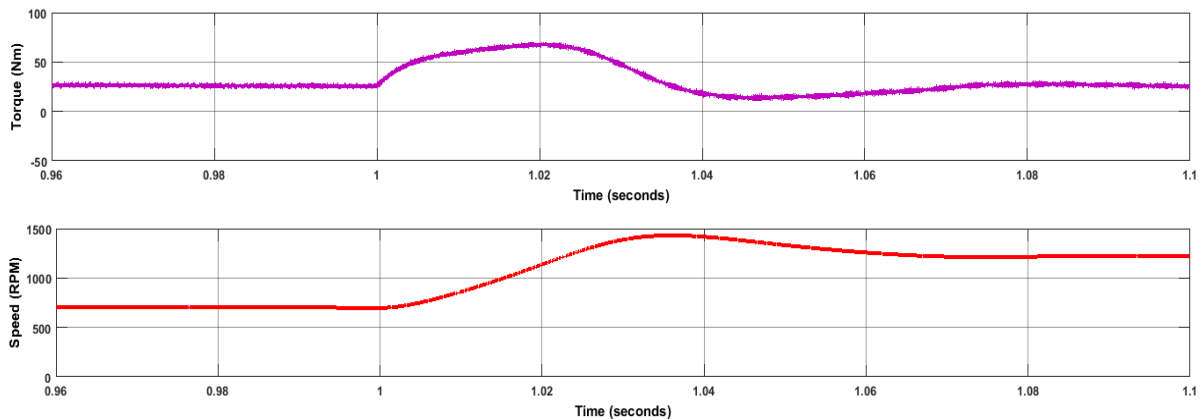


Fig. 7 Change in motor speed from 700 RPM to 1200 RPM when a PI controller is used

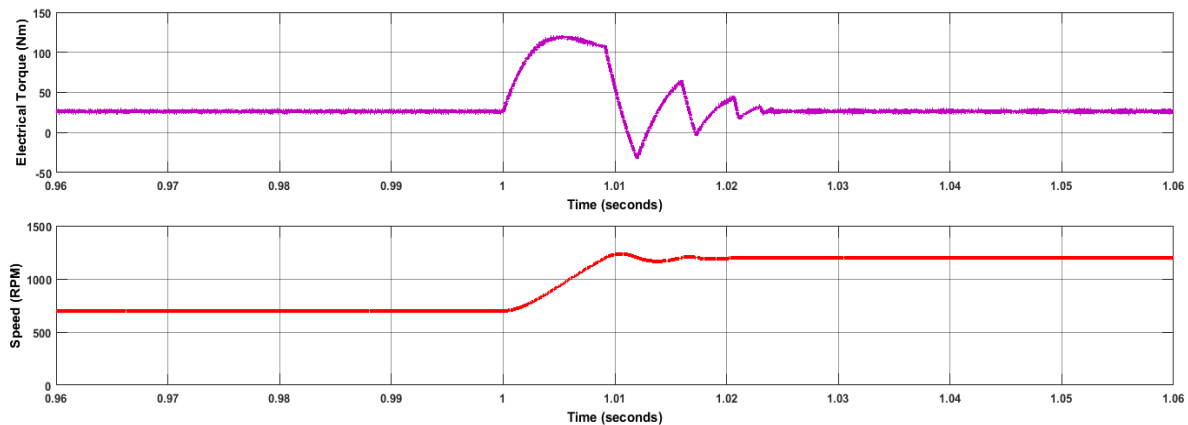


Fig. 8 Change in motor speed from 700 RPM to 1200 RPM when ISMC is used

4.3. System response to change in load torque

Another case that must be taken into consideration is the load torque change. The load torque was changed from half to full load, where the full load torque is 26 N.m. When a PI speed controller is used, the stator current of the motor increases in a smooth manner during the transient period. Also, the speed response exhibits a small dip in its value up to 200 RPM. The torque of the motor (T_e) increases as well, during the transient period. T_e shows an overshoot to approximately twice its rated value. The transient period of load change lasted for 0.15 seconds, as shown in Fig. 9. In the case of control by ISMC, the speed response shows no dip in its value during the transient period as the load is increased. T_e reaches its rated value very quickly as well. Moreover, the stator current changes immediately, but it suffers from harmonics due to a chattering phenomenon that is related to ISMC. This chattering leads to a continuous change in the control variable, which is translated to the driver frequency and modulation index. In comparison with a PI controller, ISMC in the transient period after load exhibited a change that lasted for 0.02 seconds, as shown in Fig. 10.

To overcome the issues related to chattering, several techniques can be applied. These include either increasing the switching frequency of the inverter, adding an LC filter between the inverter output terminals and the motor, or use of an unsaturated activation function for the controlling variable. Each of these solutions can be applied singly or in conjunction with others. The factors related to the enhancements are the system nature, size, and cost. Application of all the aforementioned solutions with the experimental work of this paper will be made in a future study.

4.4. Controller test for uncertainty

One of the control uncertainties is change in the DC supply voltage (Vdc) of the three-phase inverter. The change may result in a voltage above or below the rated value. The rated Vdc value that results in a three-phase 400 V RMS line to line voltage is 565 V. To check the robustness of the ISMC, the Vdc was increased to a higher value, 600 V. Then it was decreased to a lower value, 500 V, as shown in Fig. 11. In both cases, the simulation results show no effect on the steady-state values of each speed and T_e during and after the Vdc change. When PI control is used, for the same Vdc change, it can be noted in Fig. 12 that when Vdc is increased or decreased, the speed and T_e are affected. Then, after the Vdc change, the PI controller will return the motor to its desired rotational speed. In each test, the desired speed was 1000 RPM.

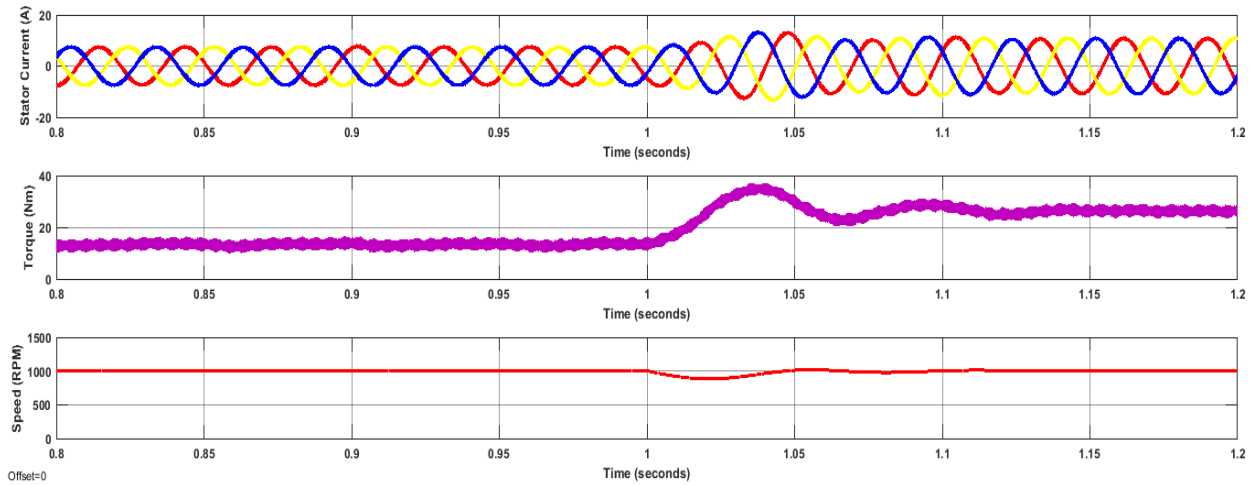


Fig. 9 Change in motor load torque from 13 Nm to 26 Nm using PI control

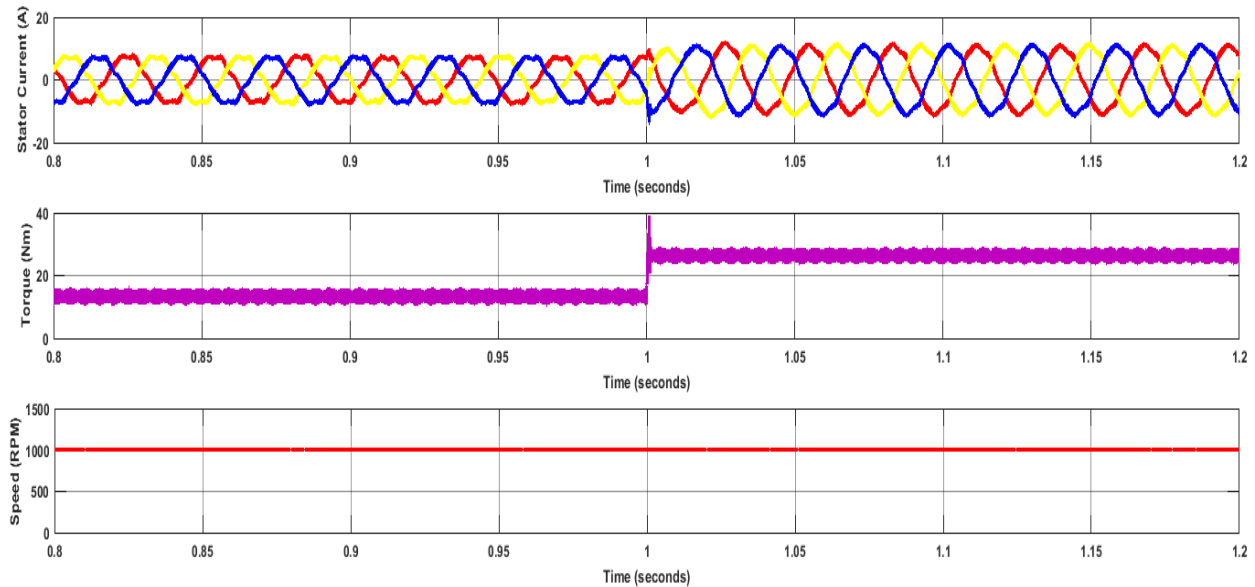


Fig. 10 Change in motor load torque from 13 Nm to 26 Nm using ISMC

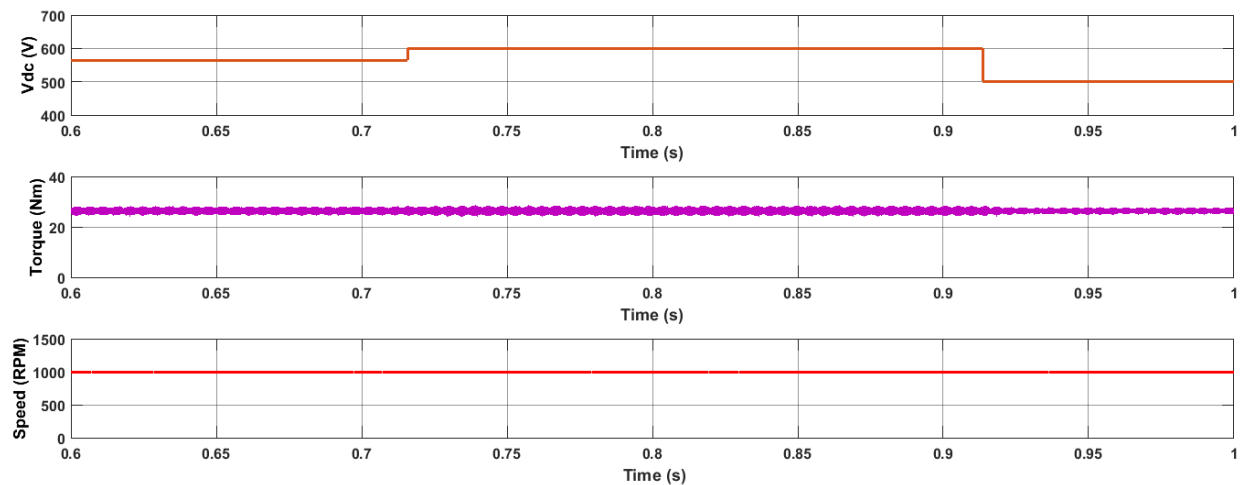


Fig. 11 System response to changes in Vdc with ISMC control

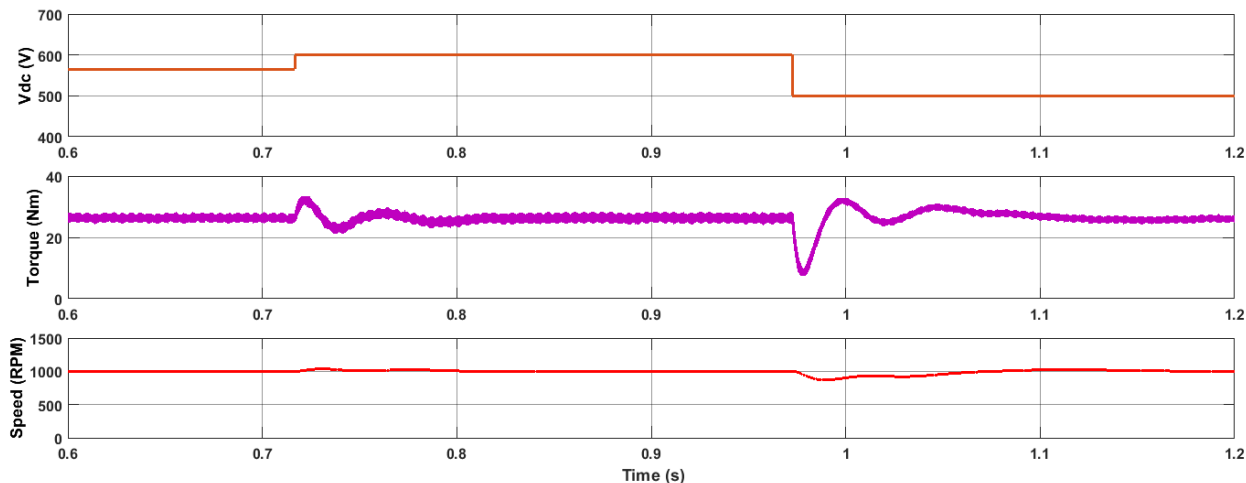


Fig. 12 System response to changes in Vdc with PI control

5. Conclusions

In this study, scalar control of a three-phase SCIM is made using PI and ISMC controllers. Numerous simulations were used to test motor performance under various operating conditions. The simulations started at a desired set point, changing the rotational speed under a constant load, changing the load, and finally changing the supplied DC voltage. The results showed that ISMC has an extremely low values for overshoot, settling time and steady-state error. These properties make it more robust and faster than a conventional PI controller. Thus, ISMC can be applied to control the speed of a three-phase SCIM in manufacturing processes, industrial applications, or in electrical vehicles that use SCIMs.

References

- [1] Chiasson J. "Dynamic feedback linearization of the induction motor", IEEE Trans. Automatic Control, Vol. 38, 1993. pp. 1588-1594.
- [2] Gopal K. Dubey, "Fundamentals of Electrical Drives", Alpha Science International LTD, India, 2001.
- [3] Bimal K. Bose, "Modern Power Electronics & AC Drives", Prentice Hall Inc., 2002
- [4] Grzegorz Tarchała, Teresa Orłowska-Kowalska, "Sliding Mode Speed and Position Control of Induction Motor Drive in Cascade Connection", Chapter 4, IntechOpen, 2016.
- [5] Joby Antony, and Akshay Kumar, "Controlling 3-Phase Induction Motors Using VFD And PLC", electronicsforu.com, 2018, URL: <https://www.electronicsforu.com/electronics-projects/control-3-phase-induction-motors-vfd-plc>
- [6] K. Venkateswarlu, G. Sandeep, N. Srinivas, K. Damodara Reddy, and A. Ramakrishna, "Speed Sensorless Sliding Mode Control of Induction Motor Using Simulink", IOSR Journal of Electrical and Electronics Engineering (IOSR-JEEE), Volume 6, Issue 2 (May. - Jun. 2013), p.p. 50-56.
- [7] Eman El-Gendy, Abdelhameed F. Ibrahim, Sabry F. Saraya, F. G. Areeed, "A Sliding Mode Controller for a Three Phase Induction Motor", International Journal of Computer Applications, Volume 64– No.11, February 2013, p.p. 33 – 39.
- [8] Swagat Pati, Sattapriya Mohanty, and Manas Patnaik, "Improvement of transient and steady state performance of a scalar controlled Induction Motor using Sliding Mode Controller", 2014 International Conference on Circuit, Power and Computing Technologies (ICCPCT), IEEE, 2014. p.p. 220-225.
- [9] Kamran Zeb, Waqar Uddin, M. A. Khan, Ayesha, Aun Haider, and H. J. Kim, "A Comparative Assessment of Scalar Controlled Induction Motor using PI, Adaptive Sliding Mode, and FLC based on SD Controllers", 2017 First International Conference on Latest trends in Electrical Engineering and Computing Technologies (INTELLECT), Karachi, Pakistan, 2017, p.p. 1-6.
- [10] Dr. Farazdaq R. Yaseen, and Walaa H. Nasser, "Speed Controller of Three Phase Induction Motor Using Sliding Mode Controller", International Journal of Computers, Communications & Control (IJCCC), Vol. 19, No. 1. March 2019. p.p. 52-62.
- [11] Divyam, Ayushi Saxena, and Bharat Singh, "Comparative Analysis of PWM Techniques and SVPWM operated V/f control of Induction Motor having different power ratings", Proceedings of the Fifth International Conference on Communication and Electronics Systems (ICCES 2020), IEEE, 2020. p.p. 6-11.
- [12] P.S. Bimbhra, "Electrical Machinery", Khanna Publishers, 2011.

- [13] Mathworks.com, “Asynchronous Machine, Model dynamics of three-phase asynchronous machine”, [URL:https://www.mathworks.com/help/physmod/sps/powersys/ref/asynchronousmachine.html?searchHighlight=asynchronous%20machine&s_tid=srchtitle](https://www.mathworks.com/help/physmod/sps/powersys/ref/asynchronousmachine.html?searchHighlight=asynchronous%20machine&s_tid=srchtitle)
- [14] P.S. Bimbhra, “Generalized Theory of Electrical Machines”, Khanna Publishers, 2011.
- [15] Muhammad H. Rashid, “Power Electronics, Devices, Circuits, and Applications”, Pearson, Education Limited, 2014.
- [16] Rajaji VD, Sekhar KC. “Power applications for fuel-cell using switching regulators”. Indonesian Journal of Electrical Engineering and Computer Science, Vol. 15 No.1, 2019; p.p. 71-9.
- [17] Axaykumar Mehta, and Brijesh Naik, “Sliding Mode Controllers for Power Electronic Converters”, Springer Nature Singapore Pte Ltd. 2019.
- [18] R. DeCarlo and S. Zak, “A Quick Introduction To Sliding Mode Control And Its Applications”, Universita’ Degli Studi di Cagliari, 2008.
- [19] Yuri Shtessel, Christopher Edwards, Leonid Fridman, and Arie Levant, “Sliding Mode Control and Observation”, Springer Science+ Business Media, New York, USA, 2014.